

See discussions, stats, and author profiles for this publication at: <https://www.researchgate.net/publication/265788239>

Geochemistry and fluoride levels of geothermal springs in Namibia

Article in *Journal of Geochemical Exploration* · January 2014

DOI: 10.1016/j.gexplo.2014.08.012

CITATIONS

8

READS

268

5 authors, including:



Ondra Sracek

Palacký University Olomouc

117 PUBLICATIONS 3,001 CITATIONS

[SEE PROFILE](#)



Heike Wanke

University of the West of England, Bristol

40 PUBLICATIONS 217 CITATIONS

[SEE PROFILE](#)



Frantisek Buzek

Czech Geological Survey

84 PUBLICATIONS 1,151 CITATIONS

[SEE PROFILE](#)

Some of the authors of this publication are also working on these related projects:



Arsenic and heavy metals in Poopó Basin, Bolivia [View project](#)



Fractionation of heavy metals and assessment of contamination of the sediments of Lake Titicaca [View project](#)



Geochemistry and fluoride levels of geothermal springs in Namibia



O. Sracek^{a,*}, H. Wanke^b, N.N. Ndakunda^b, M. Mihaljevič^c, F. Buzek^d

^a Department of Geology, Faculty of Science, Palacky University, Olomouc, Czech Republic

^b Department of Geology, University of Namibia, Windhoek, Namibia

^c Department of Geochemistry, Mineralogy, and Natural Resources, Faculty of Science, Charles University, Praha, Czech Republic

^d Czech Geological Survey, Praha, Czech Republic

ARTICLE INFO

Article history:

Received 20 April 2014

Accepted 26 August 2014

Available online 16 September 2014

Keywords:

Namibia
Geothermal springs
Fluoride
Stable isotopes

ABSTRACT

A survey of groundwater from six geothermal springs in Namibia showed high concentrations of dissolved fluoride, with values up to 18.9 mg/l. All values are higher than both the WHO limit and the Namibian guideline. High concentrations of fluoride are linked to Na-HCO₃ or Na-SO₄-HCO₃ groundwater types, with increasing sulfate and chloride concentrations towards the south of Namibia. Values of $\delta^2\text{H}$ and $\delta^{18}\text{O}$ are more negative for the north of the country, and with increasing altitude of springs and distance from precipitation sources towards the south-east from the Indian Ocean. A shift of about 1‰ from the LMWL for Windhoek was observed for $\delta^{18}\text{O}$ samples, which was probably caused by the exchange with reservoir rocks. Values of $\delta^{34}\text{S}(\text{SO}_4)$ reflect mixing of two principal sulfate sources, i.e., dissolution of gypsum originating from playas and interaction with sulfidic mineralization in tectonic bedrock zones. Values of $\delta^{13}\text{C}(\text{DIC})$ seem to be affected by a variable vegetation cover and mainly by the input of endogenous CO₂. Estimated reservoir temperatures vary from 60 °C to 126 °C, with a maximum value at the Ganigobes site. The geothermal springs of Namibia in this study do not meet drinking water standards and thus their water can be used only for other purposes e.g. for thermal spas. Treatment would be necessary to decrease dissolved fluorine concentrations for drinking water purposes.

© 2014 Elsevier B.V. All rights reserved.

1. Introduction

Namibia is a country in southwestern Africa experiencing from semiarid to extremely arid climate. This is a consequence of the cold Benguela Current flowing west of the Namibian coast. Water resources here are very scarce and water supply is of a serious concern. In coastal zone harvesting of water condensed from fog is a standard practice (Shanyengana et al., 2002). Thermal waters in Namibia have been known as early as 1837 at the capital Windhoek, locally known by the Nama people as Ai=//gams (fire water) and by the Herero people as Otjomuise (the place of smoke). Geothermal waters discharge in several springs in Namibia, usually located on tectonic lines. Locations of the springs included in this study are given in Fig. 1a. High concentrations of fluoride may represent a problem for exploitation of geothermal waters in the country.

Fluorine occurrence is widespread in the lithosphere as a component of rocks and minerals. The earth's crust contains abundant fluorine in calcium granite (520 ppm), low calcium granite (850 ppm), alkaline rocks (1200–8500 ppm), shale's (740 ppm), sandstone (270 ppm), deep sea clay (1300 ppm), and in deep sea carbonates (540 ppm) (NEERI, 1985). Fluorine is sparingly soluble in water, hence due to its highly electronegative characteristics it forms only fluorides and no

other oxidation states are found in natural water (Hem, 1992). Fluorite (CaF₂) is the principal rock-forming mineral that has fluorine as an essential constituent and has generally been considered as a dominant source of groundwater fluorine, especially in granitic terrain. Fluoride concentration in groundwater is frequently proportional to the degree of water–rock interaction because fluoride primarily originates from geological sources (Banks et al., 1995; Carillo-Rivera et al., 2002; Gizaw, 1996). The potential geogenic sources of fluoride in groundwater include various soils and minerals in rocks, such as topaz, fluorite, fluorapatite, cryolite, amphiboles, and micas (Bardsen et al., 1996; Handa, 1975; Pickering, 1985; Subba Rao and Devadas, 2003; Wenzel and Blum, 1992).

Apatite is present in sedimentary rock and fluorite often occurs as a cementing material in sediments. A positive correlation between fluoride and dissolved silica as well as between fluoride and sodium also supports the silicate origin of fluoride (Chae et al., 2006; Koritnig, 1992). However, quantitative assessments of fluoride enrichment in natural waters, especially through the study of fluid–mineral equilibria, are sparse (Saxena and Ahme, 2001).

Fluoride belongs to a family of so-called geogenic contaminants: its enrichment in water is not generally a consequence of human activities (Johnson et al., 2011), but rather natural processes. It is a serious problem in many countries including Ethiopia (Tekle-Haimanot et al., 2006), Kenya (Gaciri and Davies, 1993), India (Jacks et al., 2005), Sri Lanka (Dissanayake and Chandrajith, 2007), Mexico (Armenta and Segovia,

* Corresponding author. Tel.: +420 585634537; fax: +420 585225737.
E-mail address: srondra@yahoo.com (O. Sracek).

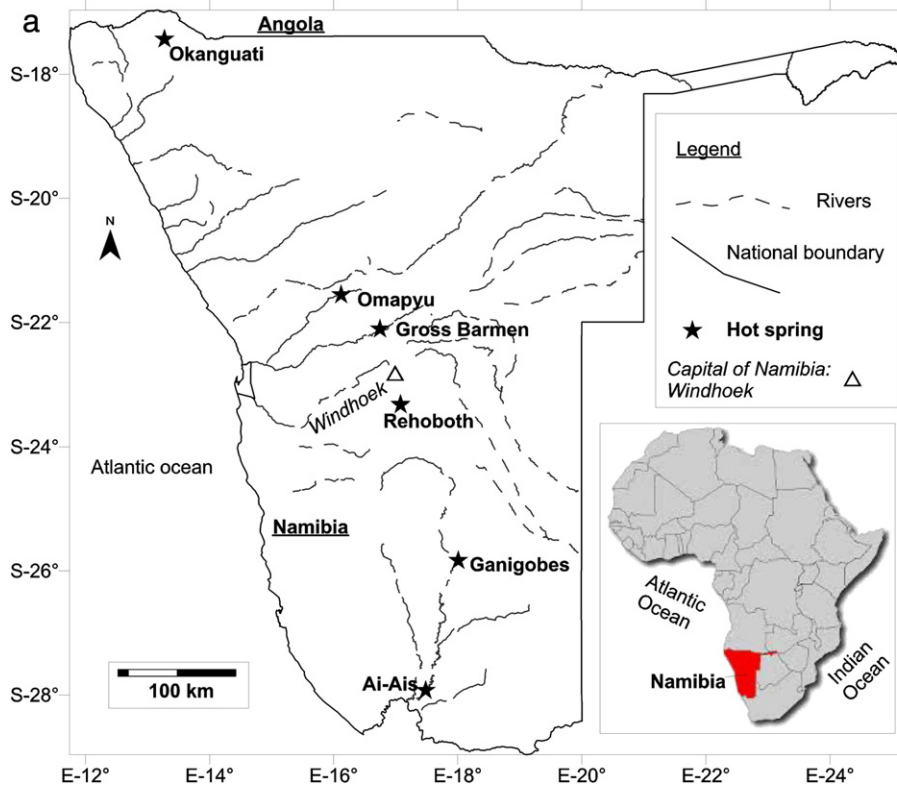


Fig. 1. (a) Location of sampled geothermal springs in Namibia, (b) geological map of Namibia. (adapted from Petzel and Schreiber, 1999)

2008), and Argentina (Bhattacharya et al., 2006). Its high concentrations are generally linked to high residual alkalinity ($\text{Ca}^{2+} < \text{HCO}_3^-$), high Na^+ , and high pH waters (Jacks et al., 2005; Sracek and Hirata, 2002). In high Ca^{2+} waters fluoride precipitates as fluorite (CaF_2) which generally controls maximum fluoride concentration in waters.

The maximum tolerance limit of fluoride in drinking water specified by the World Health Organization, (WHO, 1998), is 1.5 mg/l. However, fluorine is also essential for human beings as it helps in normal mineralization of bones and formation of dental enamel. It adversely affects human health when its concentration exceeds the limit of 1.5 mg/l. In some countries, fluorine is added to water in small amounts to prevent health hazards. However, ingestion of water with fluoride concentrations above 1.5 mg/l results in dental fluorosis characterized initially by opaque white patches, staining, mottling, and pitting of teeth (Kundu et al., 2001). In an advanced stage, deformation of bones occurs because fluorine in human body interferes with the metabolism of calcium (Rango et al., 2012).

Skeletal fluorosis may occur when fluoride concentrations in drinking water exceed 4–8 mg/l, which leads to an increase in bone density, calcification of ligaments, rheumatic or arthritic pain in joints and muscles along with stiffness and rigidity of the joints, bending of the vertebral column, and so on. Fluoride has the same effect on livestock as in humans, with concentrations above 2 mg/l affecting animal breeding and causing mottled teeth in young animals. The bone joints of some animals may become swollen and painful resulting in shifting lameness, stiffness of joints and backbones (Sudarshan and Rajeswara Reddy, 1991). High concentration of fluoride in irrigation water prevents the accumulation of chlorophyll in plant leaves.

Other geothermal species of concern in the Namibian springs are boron, uranium and especially arsenic. In geothermal reservoirs, arsenic is generally present in Na-Cl type of water in acid igneous rocks (Birkle et al., 2010; López et al., 2012; Webster and Nordstrom, 2003).

The main objective of the study was to explain the geochemical and isotopic composition of the geothermal waters in Namibia including levels and behavior of fluoride.

2. General geology and description of spring sites

In Namibia a total of 24 springs are reported as thermal, of which nine are scalding (Kent, 1949). Six out of these springs were sampled for this study: the springs in Rehoboth, Gross Barmen, Ganigobes, Omapyu, Okanguati, and Ai-Ais (Fig. 1a). Several other springs could not be sampled as groundwater levels had dropped and springs stopped discharging (e.g. springs in Windhoek).

Geological map of the study area is shown in Fig. 1b. Most hot springs in Namibia are situated within areas dominated by the Damara Orogenic belt which forms a part of the Pan-African tectono-thermal belts that surround and dissect Africa. The Damara Orogen occurred during the Neoproterozoic and early Paleozoic between 750 and 450 Ma ago (Schneider, 2008). According to Miller (2008), the Damara Belt consists of the NNW trending coastal arm, the Kaoko Belt which extends into Angola and continues northward and has a NE trending arm, and the Damara Belt, which extends through central Namibia across northern Botswana to the Zambezi Belt and the Mozambique Belt.

The Damara Belt was formed during the collision between the Congo Craton in the north and the Kalahari Craton in the south. During the collision, the Kalahari Craton was subducted underneath the Congo Craton, and it was accompanied by major deformation, metamorphic and intrusion events.

The Damara Belt shows well-preserved bivergent symmetry typical for collisional belts. Based on lithological, structural and metamorphic characteristics, the Damara Belt is subdivided into contrasting tectonostratigraphic zones from the north to the south, into the Northern Platform, Northern Marginal Zone, Northern Zone, Central Zone,

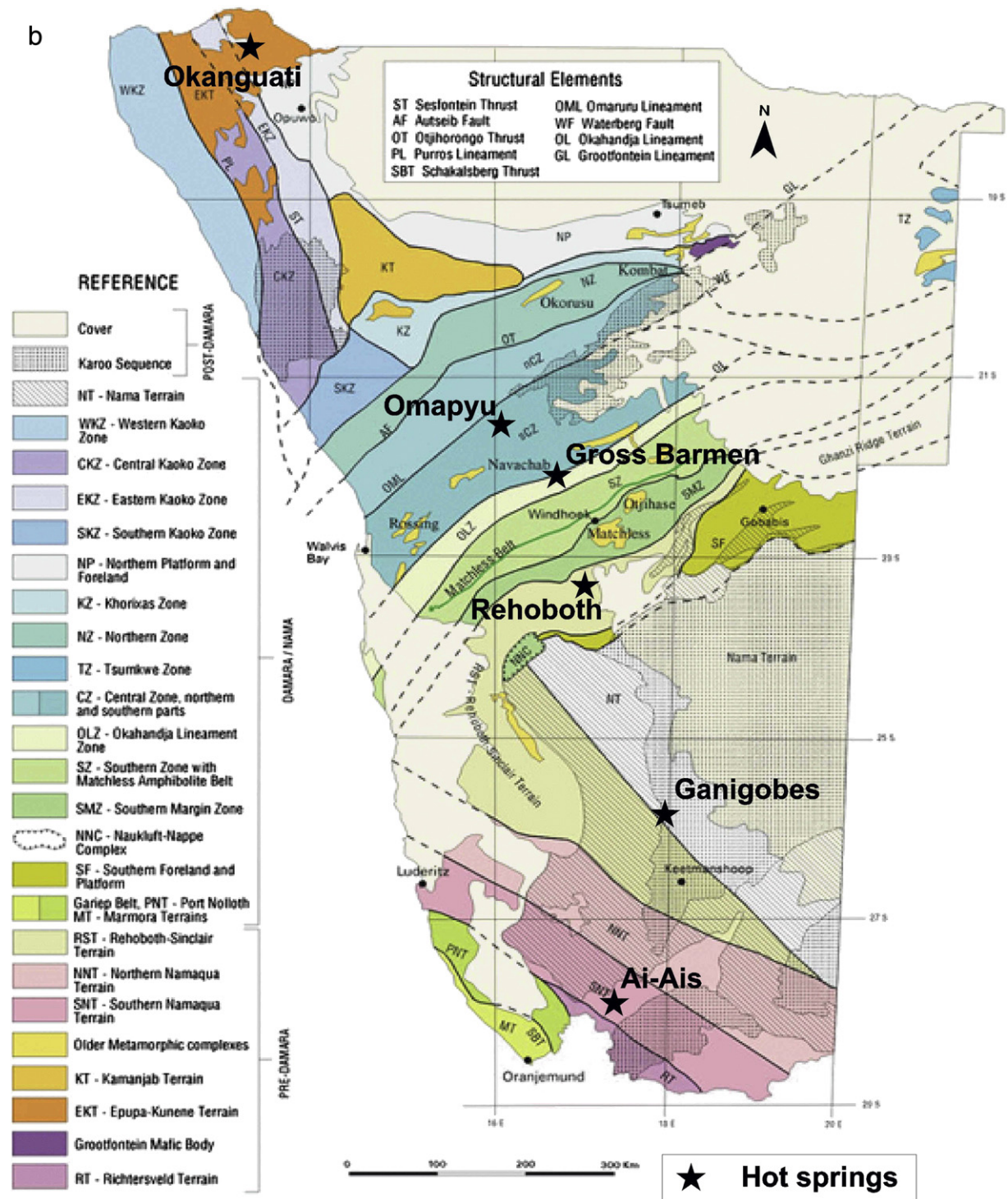


Fig. 1 (continued).

Okahandja Lineament Zone, Southern Zone, Southern Marginal Zone, Southern Foreland, and Southern Platform.

The hot springs at Omapyu and Gross Barmen, (Fig. 1b), are located in the Central Zone of the Damara Belt, bordered by the Otjohorongo thrust at the north and the Okahandja lineament at the south (Miller, 1983). The Central Zone is a high-temperature–low-pressure zone of the orogen and is characterized by sillimanite–cordierite metamorphic assemblages, numerous granitic plutons, and fold structures. The Central Zone is divided into a northern Central Zone and a southern Central Zone, separated by the NE trending Omaruru Lineament along which

the lower Swakop Group rocks thicken rapidly northward (Miller, 2008). The southern part of the Central Zone is characterized by much deeper levels of exposure and the units present are pre-Damara basement gneiss, the Nosib and Swakop Groups.

The hot spring of Okanguati, (Fig. 1b), is located in the Northern Platform and Foreland Zone in the Kunene region in north-western Namibia (Fig. 1b), with the granitic and gneissic rock types covering the vast areas in the Kaokoveld (Miller, 1983). The mountain ranges of carbonate rocks related to the Otavi Mountain Land form the eastern edge of the area. The Okanguati spring is situated in the mountainous and

deformed Kaokoland and the thermal spring discharges from deformed para- and ortho-gneiss. Climate at the site is semiarid and the spring is located at upper slope of a valley. The local habitants use this water for washing and also collect it for domestic purposes including drinking water.

The Omapyu hot spring, (Fig. 1b), flows through fine to medium grained syn- to post-tectonic leuco-granites (Fig. 1b). At the Omapyu, the spring is captured 1 m below the topographic surface, in a 1 m diameter well and from there it is pumped into a swimming pool. Situated east of the Erongo Complex, the spring is situated in a fault system in the syn- to post-tectonic related to the Damara orogeny).

The Gross Barmen spring, (Fig. 1b), is located in the Kuiseb Formation of the Swakop Group containing mica schists, deep seated fault systems and granite intrusions. The water discharging from this spring is piped to the Gross Barmen Spa which is currently under renovation. Climate at Omapyu and Gross Barmen sites is semiarid and springs are located at a plain without significant topographical features in their proximity, suggesting a role of free convection in the springs' discharge.

In Rehoboth, the hot spring, (Fig. 1b), is located close to the Roman Catholic hospital. The spring is captured and the hot water is collected for domestic use. The hot spring at Rehoboth was also used to run a spa which is currently under reconstruction. The four formations outcropping at Rehoboth area are: Elim Formation consist of sedimentary rocks and slightly metamorphosed basic lavas; Marienhof Formation: quartzites, phyllites, basic lavas, and acid volcanic rocks; Billstein Formation: quartzite, phyllite with many beds of basic lavas; and Gaub Valley Formation: consists of brown quartzites, phyllites, brown limestones, and conglomerates, acidic and basic lavas. In addition, intrusions of gabbro, pyroxenites, serpentinites, diorites and granodiorites are found here. Climate at the site is semiarid and the spring is located in a river valley.

The Ai-Ais spring, (Fig. 1b), is described as a scalding hot spring by Kent (1949). It discharges from basic, neutral or acid volcanic rocks, originating about 800 million years ago, with intrusions of granodioritic and porphyritic rocks from a deep reaching fault system. The spring is located in arid southern Namibia at a bottom of valley surrounded by mountains. The spring water is used in a local spa.

In Ganigobes spring (Fig. 1b), situated at the southern end of the Fish River Canyon, a circular wall is built around the hot spring and the overflowing water flows to the Fish River. The spring water is used for recreation purposes. The spring discharges from the Dwyka Formation overlain by argillaceous schists, sandstones and coal bearing schists of the Ecca Group. Red deposits and aeolian sands of the Karoo followed by Cretaceous basalts are estimated to be from 180 to 120 ma old. The volcanic rocks are dissected by large dykes. The sediments in the Ganigobes area make up the base of the Dwyka series (Carboniferous–Permian) (Kent, 1949). Climate at the site is arid and the spring is located at a plain. The Brukkaros volcanic structure surrounded by carbonatite dykes and pipes, (Schneider, 2008), is located relatively close.

3. Material and methods

Sampling was performed in January 2013. Temperature, pH, oxidation–reduction potential (ORP), and electrical conductivity (EC) were measured on-site. The samples for the analysis were stored in high density polyethylene (HDPE) bottles, pre-filtered with 0.45 µm Millipore filters, acidified for cations with HNO₃–Suprapur, and analyzed with the ICP-MS technique. Arsenic concentrations in geothermal fluids were determined with the Atomic Absorption Spectrometry with hydride generation. Anions were determined by high performance liquid chromatography (HPLC), (Dionex ICS 2000). Precision of individual measurements was ± 5%. Alkalinity was determined by titration with HCl using the Gran plot to determine the end point. Water chemistry analyses have been performed at Faculty of Science, Charles University in Prague, Czech Republic.

Samples for stable isotopes of water were stored in air-tight sealed glass bottles. Isotope values δ¹⁸O and δ²H in water were determined at the Czech Geological Survey in Prague, Czech Republic, using a Los Gatos Research laser absorption spectrometer. The reproducibility of measurements was 0.5‰ for δD and 0.08‰ for δ¹⁸O. Precipitates for ¹³C–CO₃²⁻ analyses were prepared by adding NaOH and BaCl₂ and then the precipitate was filtered out. In next step, the BaCO₃ precipitate was dissolved by H₃PO₄ according to McCrea (1950), and δ¹³C was measured with a precision better than 0.05‰.

Sulfate sulfur from waters was precipitated with BaCl₂ (in hot solution acidified with HCl to pH 3.5) as BaSO₄ which was decomposed with a mixture of V₂O₅, SiO₂ and Cu at 1000 °C in a vacuum to SO₂ according to Yanagisawa and Sakai (1983). Reproducibility of δ³⁴S preparation and measurement is ± 0.25‰. Calibration of the laboratory standard was carried out by the IAEA international standards (NZ1 and NZ2) and the recommended comparative materials (NBS122 and NBS127).

Speciation calculations were performed by the program PHREEQC (Parkhurst and Appelo, 1999) using the databases minteq.dat available together with PHREEQC. The Na–Li geothermometer for low chloride waters, (Fouillac and Michard, 1981), expressed as

$$t^{\circ}\text{C} = \frac{1000}{0.389 + \log(m\text{Na}/m\text{Li})} - 273.15$$

was used for evaluation of the reservoir temperatures. Several other geothermometers including Na–K and Na–K–Ca have been tested, but they gave inconsistent results, probably due to the cation exchange impact.

4. Results

4.1. Water chemistry

4.1.1. Field parameters

The results for field parameters are given in Table 1.

Temperatures of the studied springs varied from 24.7 up to 60 °C. Assuming a geothermal gradient of 33 °C/km for Namibia (Kent, 1949) and that the area is non-magmatic, the water in the hot springs have reached a depth of about 2000 m below ground surface (bgs). The electrical conductivity (EC) of the samples varies from 1.1 to 4.4 mS/cm. The pH of the sampled springs was between 6.94 and 8.08. The samples from hot springs have redox potential (Eh) values ranging from 39 to 360 mV_H, indicating post-oxic or moderately reducing redox status of waters.

4.1.2. Major ions

Major ion concentrations are also in Table 1 and spring waters are plotted in the Piper diagram in Fig. 2. The Piper plot shows that cations in the springs generally plot in the sodium plus potassium field. Most anions in the Piper plot show that the springs generally do not plot in a dominant anion region, but there seems to be a transition from HCO₃⁻ to SO₄²⁻ field.

The Omapyu and Okanguati hot springs are of the Na–HCO₃ type and both samples from Gross Barmen show similar patterns and are of Na–SO₄–HCO₃-type. In the Rehoboth hot spring, the water is of Na–SO₄–HCO₃ type. The Ganigobes spring is of mixed Na–SO₄–Cl–HCO₃ type. The Ai-Ais hot spring has water of Na–SO₄–Cl type.

In general, springs south of Windhoek have higher sulfate concentrations than the springs north of Windhoek (maximum of 814 mg/l at Rehoboth) and this applies also to chloride concentrations (maximum of 475 mg/l at Ai-Ais and similar concentration at Ganigobes). Sodium is the dominant cation in all springs (maximum 684 mg/l at Ganigobes), but the spring at Ai-Ais also has relatively high calcium concentration of 130 mg/l.

There are increased nitrate concentrations at Ai-Ais, Omapyu and especially at Ganigobes (Table 1). Geogenic origin of nitrate is unlikely

Table 1
Field parameters, major ions and NO_3^- concentrations in mg/l, n.a. – not available.

Spring	Latitude	Longitude	Altitude (m)	pH	T (°C)	Eh (mV _H)	EC (mS/cm)	K ⁺	Na ⁺	Ca ²⁺	Mg ²⁺	Cl ⁻	SO ₄ ²⁻	HCO ₃ ⁻	NO ₃ ⁻
Rehoboth	S23°19.445'	E017°04.706'	1401	6.94	59.6	39	4.37	56.4	381	32.8	5.9	133	814	360	<2
Gross Barmen Ditch	S22°06.690'	E016°44.808'	1219	7.47	48	40	2.4	20.1	245	17.8	1.6	106	311	340	<1
Gross Barmen Chamber	S22°06.651'	E016°44.774'	1219	7.58	70	n.a.	2.37	20.5	249	31.3	3.6	103	306	352	<1
Ganigobes	S25°50.051'	E018°00.520'	929	7.42	43.7	360	3.26	0.07	684	47	16.7	472	714	436	34.5
Omapyu	S21°33.525'	E016°07.275'	1301	7.21	47.4	360	2.11	0.3	307	17.4	1.1	117	140	406	5.4
Ai-Ais	S27°55.717'	E17°29.0'	1202	7.28	60	n.a.	2.62	0.18	550	130	3.6	475	742	124	13.3
Okanguati	S17°27.698'	E13°14.714'	1083	8.08	42.2	n.a.	1.134	10	250	8.8	1.2	118	106	213	<1

and the presence of nitrate probably indicates mixing with shallow aquifer groundwater.

4.1.3. Trace elements and geothermal indicators

Concentrations of trace elements and geothermal indicators are presented in Table 2 and in Fig. 3. Concentrations of F⁻ range from 2.1 mg/l (Ganigobes) to 18.9 mg/l (Omapyu). This is amongst the highest fluoride concentrations occurring in groundwater in Namibia, and only 23 samples out of 27,736 hydrochemical analyses stored in the Namibian groundwater database GROWAS, managed by the Department of Water Affairs, exceed this remarkably high value recorded at Omapyu. These values are comparable to those at the Ethiopian Rift (Tekle-Haimanot et al., 2006).

These values are high for Namibia, where approximately 11% of all available hydrochemical analyses for groundwater exceed the national permissible value of 2 mg/l for classifying waters as class A (water of excellent quality) and class B (good quality).

It can be observed in Fig. 3 that total concentrations of Li, Sr, B, Mn, Mo, Ba, and U are elevated in the springs and that Be, Cr, Co, Y, Ag, La and Bi seem to occur at low concentrations relative to the other

elements. A relatively higher concentration of U, 25.57 µg/l, is observed in the Ganigobes hot spring. Strontium occurs at higher concentrations than Ba. Fluorine is the major concern to human health in the tested geothermal waters. However, the WHO (1998) guideline values for permissible concentrations in drinking water are also exceeded in Ai-Ais for boron (guideline value 500 µg/l), in Rehoboth for arsenic (guideline value 10 µg/l) and in Ganigobes for boron, arsenic, selenium (all guideline values 10 µg/l) and uranium (guideline value 15 µg/l).

4.2. Isotopes

Concentrations of stable isotopes are summarized in Table 3. Values of $\delta^2\text{H}$ and $\delta^{18}\text{O}$ are also plotted in Fig. 4 and show a deviation from the Windhoek meteoric water line ($\delta^2\text{H} = 7 \delta^{18}\text{O} + 8$; derived from the IAEA GNIP station in Windhoek). The two southern-most springs Ai-Ais and Ganigobes show least negative values while the data from the springs in northern and central Namibia plot closer together and have more negative values. The regression line for the hot spring data shows a shift of about 1‰ to the right from the meteoric line and thus towards enriched values of $\delta^{18}\text{O}$. Such a shift can be attributed to the

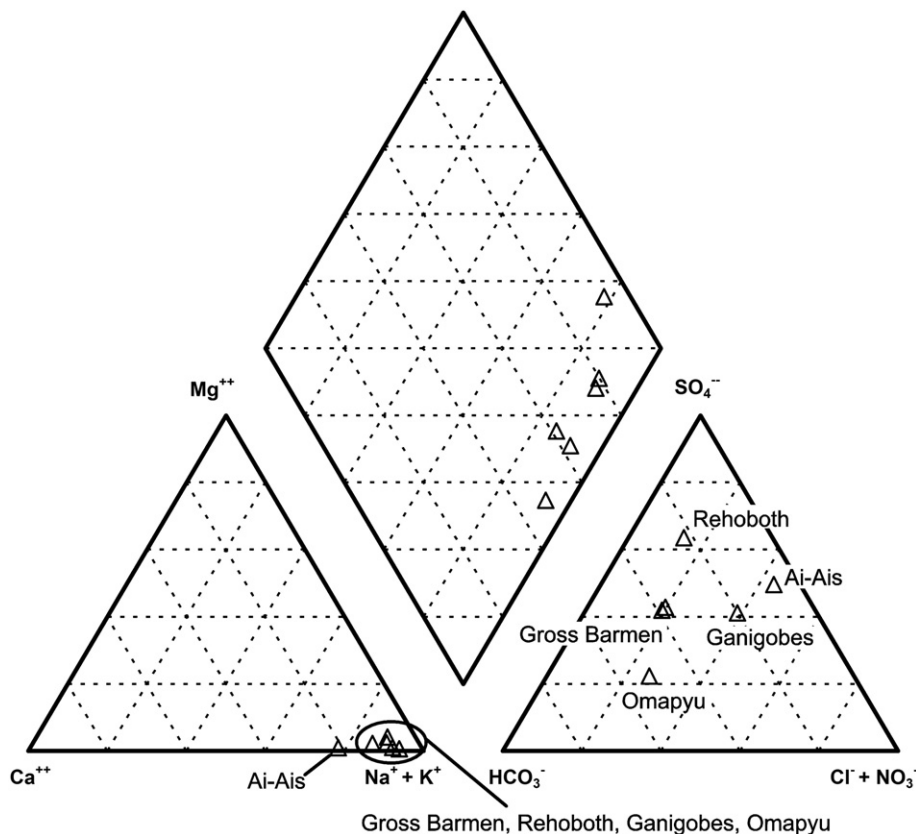


Fig. 2. Piper diagram of geothermal spring waters.

Table 2

Trace elements, concentrations in $\mu\text{g/l}$, F^- and Fe in mg/l , Okanguati sample with F^- concentration of 13 mg/l is not included due to missing data.

Element	Spring					
	Rehoboth	Gros Barmen chamber	Gross Barmen ditch	Ai-Ais	Ganigobes	Omapyu
F	9.57	7.2	6.9	6.15	2.1	18.9
Fe	0.13	0.09	0.01	0.43	0.45	0.09
Li	279.4	183.2	177	464.5	1587	369.9
Be	1.123	0.285	0.157	0.456	0.192	1.382
B	121	183	189	1038	2296	319.6
Sc	13.81	11.73	11.35	8.45	2.92	13.41
Ti	9.06	8.676	7.786	15.54	17.2	10.49
Cr	0.334	0.29	0.429	0.996	1.576	1.231
Mn	52.46	42.19	6.112	108.8	12.31	59.66
Co	0.051	0.049	0.047	0.312	0.288	0.096
Ni	0.869	0.653	0.71	3.26	3.124	0.676
Cu	0.287	0.498	3.101	6.41	3.574	2.128
Zn	12.57	5.731	4.286	15.43	10.72	4.137
As	21.24	1.273	3.457	4.972	28.35	7.041
Se	3.337	1.893	2.021	4.544	14.21	1.532
Sr	1409	471.9	605.1	2374	3855	154
Y	0.022	0.044	0.025	0.259	0.43	0.055
Mo	12.18	0.692	1.012	18.37	9.965	0.53
Ag	0.106	0.207	0.018	0.056	0.074	0.033
Cd	0.057	0.025	0.023	0.223	0.35	0.018
Sb	2.696	0.271	0.057	0.808	0.167	0.407
Ba	32.54	27.88	41.04	48.46	39.33	9.768
La	0.041	0.062	0.03	0.347	0.298	0.106
Ce	0.017	0.105	0.043	0.545	0.386	0.154
Tl	1.09	0.43	0.413	0.366	0.053	5.053
Pb	0.024	0.052	0.05	0.84	0.67	0.414
U	0.067	0.039	0.075	1.838	25.57	0.031

exchange between water and rocks at elevated temperatures (Clark and Fritz, 1997), as the hydrogen isotope remains unaffected because of low hydrogen content in the reservoir rocks. However, the impact of evaporation is also possible in some samples, e.g. Rehoboth. If these waters were from the last glacial period, the observed shift to the right might be a consequence of lower deuterium excess in a drier climate (Clark and Fritz, 1997). There are no available data on the waters' age, but a glacial age is unlikely because the observed continental effect is consistent with a modern precipitation pattern, i.e., with the origin of precipitation in the SE from the Indian Ocean. On the other hand, during the last glaciation the precipitation originated in the Atlantic Ocean area due to a different air mass circulation (Gasse, 2000; Lancaster, 1988; Stute and Talma, 1998; Talma and Vogel, 1983).

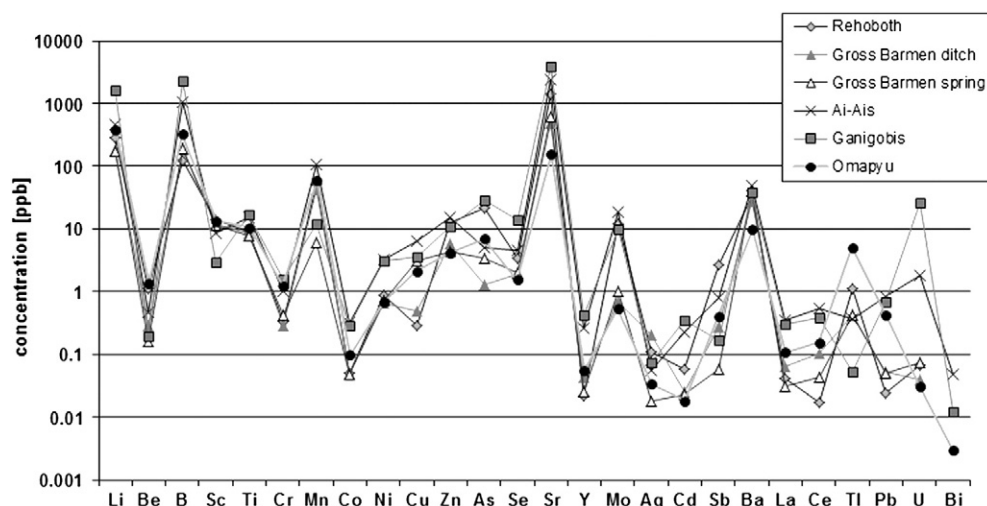
Table 3

Stable isotopes ratios for hot springs in Namibia (na – not analyzed).

Sample/value	$\delta^2\text{H}$ [‰]	$\delta^{18}\text{O}$ [‰]	$\delta^{13}\text{C}$ (DIC) [‰]	$\delta^{34}\text{S}$ (SO_4) [‰]
Gross Barmen ditch	−53.7	−7.6	−6.8	22.8
Gross Barmen spring	−55.6	−7.9	−5.7	21.7
Rehobot spring	−56.2	−8.2	−4.7	12.8
Ai-Ais spring	−36.6	−5.2	na	na
Ganigobes	−40.6	−5.7	−10.3	6.6
Omapyu	−51.5	−7.4	−4.9	18.9
Okanguati 1	−50.6	−7.3	na	na
Okanguati 2	−50.8	−7.3	na	na

When the spring waters were compared to the elevation at which they were taken from, the least negative values are associated with the lowest altitude and the highest altitudes with the most negative values. This is likely to be caused by an altitude effect on precipitation. However, the altitude effect is combined with the already mentioned continental effect because the precipitation in Namibia originates in the Indian Ocean and travels a considerable distance before reaching Namibia (Stute and Talma, 1998). Precipitation originating in the Atlantic Ocean is negligible, but there can be some contribution of water condensed from the fog originating in the coastal area (Shanyengana et al., 2002). In Fig. 4, the two springs with the least negative values are Ganigobes and Ai-Ais, both in southern Namibia, which are at lower altitude compared to Rehoboth and Gross Barmen. Both springs are also located in southern Namibia, where the precipitation pattern (winter rain) is different from the central and northern parts of Namibia (summer rain).

Values of $\delta^{34}\text{S}$ (SO_4) are in Table 3 and are plotted vs. concentrations of sulfate in Fig. 5. The range of values is from 6.6‰ to 22.8‰. Samples with relatively low concentrations of SO_4^{2-} are enriched in $\delta^{34}\text{S}$ (SO_4) isotopes. This suggests that sulfate reduction may have taken place in isotopically enriched samples (Clark and Fritz, 1997). However, samples are from different reservoirs and sulfate origin may be different from a simple sulfate reduction pathway. The Damaran bedrock sulfides show a large range of $\delta^{34}\text{S}$ values from −4.1 to +13.8‰ (Eckhardt and Spiro, 1999) and relatively low $\delta^{34}\text{S}$ (SO_4) values in some springs may be caused by interaction of water with sulfidic mineralization. Other samples have relatively lower sulfate concentrations and enriched $\delta^{34}\text{S}$ (SO_4) values e.g. Omapyu at Gross Barmen. The enriched values are probably caused by a relatively higher proportion of sulfate from dissolution of evaporates precipitated at playas with values of $\delta^{34}\text{S}$ (SO_4) up to 20.8‰ (Eckhardt and Spiro, 1999). Thus, the $\delta^{34}\text{S}$ (SO_4) variability reflects a different proportion of sulfate from two mentioned principal sources.

**Fig. 3.** Concentrations of trace elements.

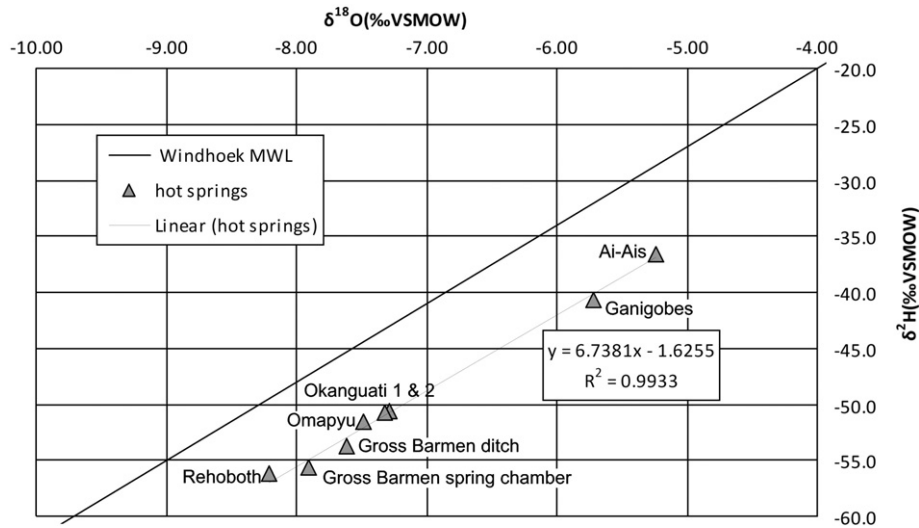


Fig. 4. Plot of $\delta^2\text{H}$ vs. $\delta^{18}\text{O}$.

The range of $\delta^{13}\text{C}(\text{DIC})$ values is from -4.7 to -10.3% . Surprisingly, the highest bicarbonate concentrations correspond to the most isotopically negative samples (Fig. 6). This is in contradiction with common observations of an opposite trend in thermal waters (Dupalová et al., 2012; Noseck et al., 2009). Again, the commonly observed trend applies to a single reservoir structure, but here we deal with reservoirs separated by several hundred kilometers. The most negative values of -10.3% at Ganigobes can be caused by some input of carbon from decomposition of organic matter with $\delta^{13}\text{C}$ about -27% (Clark and Fritz, 1997). In contrast, maximum values of -4.7% and -4.9% at Rehoboth and Omapyu may be linked to the input of endogenous CO_2 with values of $\delta^{13}\text{C}$ of about -3.0% (Dupalová et al., 2012). All samples are within the range of values observed at the Ethiopian Rift from -14.7% to -2.1% , where the input of endogenous CO_2 is important (Bretzler et al., 2011).

Considering the $\delta^{13}\text{C}$ for Ganigobes is in the range of -10% and for all other springs in the range of -5% , it might also reflect the different rain regimes (summer and winter rain), subsequently different vegetation composition and isotopic composition of root zone CO_2 . In addition, the Ganigobes site has the lowest mean annual precipitation compared to all other sampled sites and, thus, the abundance of C3 and C4 plants can be different.

4.3. Speciation calculations

Saturation indices for selected minerals are given in Table 4. Samples at Ai-Ais, Ganigobes, and Okanguati are supersaturated with respect to calcite. At Ganigobes, supersaturation is also reached for dolomite. The

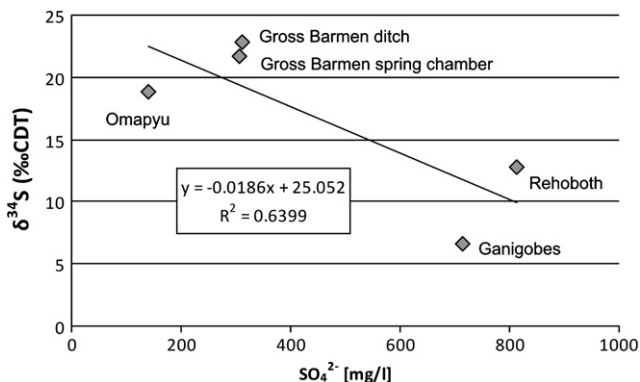


Fig. 5. Plot of $\delta^{34}\text{S}(\text{SO}_4)$ vs. sulfate concentrations.

samples supersaturated with respect to calcite are also supersaturated with respect to barite. On the other hand, all samples are undersaturated with respect to gypsum, in spite of relatively high sulfate concentrations in some springs. Supersaturation with respect to fluorite is reached at Omapyu and Okanguati, but other samples are close to saturation except the Ganigobes sample. Most samples are supersaturated with respect to $\text{Fe}(\text{OH})_3$, but saturation indices for this phase are uncertain due to an uncertain redox status. All calculated $\log P_{\text{CO}_2}$ values except for the Okanguati sample value are > -2.0 with a maximum of -1.17 at Rehoboth. These values are much higher than the atmospheric value of -3.5 suggesting some input of endogenous CO_2 because desert soils are relatively poor in organic matter.

5. Discussion

Most sample springs have Na as the principal cation and HCO_3^- or SO_4^{2-} as the dominant anion, and SO_4^{2-} concentrations increase towards south. In the Ganigobes spring, there is no dominant anion. The Na- HCO_3 water type can be formed by two principal processes: (1) Interaction of CO_2 with silicates such as albite (Toran and Saunders, 1999), and (2) dissolution of carbonates such as calcite coupled to cation exchange of released Ca^{2+} for Na^+ on exchange sites (Sracek and Hirata, 2002). Both processes generally cannot be distinguished on the basis of $\delta^{13}\text{C}(\text{DIC})$ values because CO_2 involved in the dissolution of silicates and carbonates have similar $\delta^{13}\text{C}$ values (Dupalová et al., 2012). The reaction path (1) is probably dominant, but reaction (2) may also play a role because geothermal shift for stable isotopes and relatively low Ca^{2+} and increased SO_4^{2-} concentrations suggest a

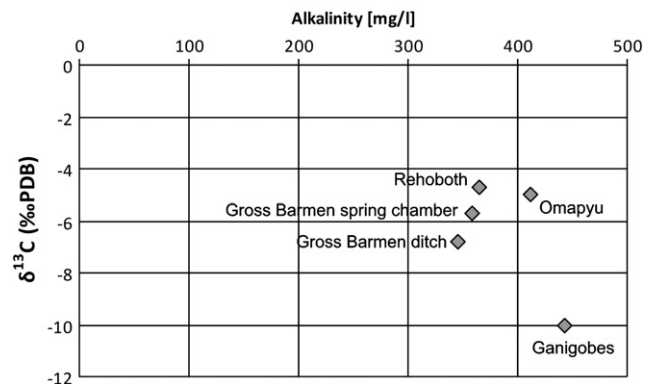


Fig. 6. Plot of $\delta^{13}\text{C}(\text{DIC})$ vs. alkalinity.

Table 4
Saturation indices for selected minerals and log P_{CO_2} values (na – not available).

Spring/SI value	Calcite	Dolomite	Barite	Gypsum	Fe(OH) ₃	CaF ₂	Log P_{CO_2}
Rehoboth	−0.33	−1.01	−0.05	−1.33	−1.92	−0.04	−1.17
Gross Barmen	−0.09	−0.76	−0.18	−1.83	na	−0.29	−1.81
Ai-Ais	0.16	−0.83	0.07	−0.82	0.55	−0.16	−1.99
Ganigobes	0.20	0.37	0.11	−1.30	1.42	−1.09	−1.71
Omapiyu	−0.24	−1.17	−1.87	−2.14	0.51	0.59	−1.47
Okanguati	0.03	−0.34	na	−2.50	na	0.07	−2.66

presence of carbonates and cation exchange, respectively. This reaction path may also lead to the precipitation of calcite and, thus, high mobility of fluoride due to low Ca^{2+} concentrations. Increasing SO_4 concentrations towards the south are probably caused by some recharge of the spring water from the playas covered by sulfate mineral crusts, (Eckhardt and Spiro, 1999), because the degree of aridity and the amount of pedogenic gypsum and other sulfate minerals also increases towards south. However, the recharge from playas seems to be limited because concentrations of Ca^{2+} are < 100 mg/l except in the Ai-Ais sample.

Geothermal waters were recharged as meteoric waters originating from the Indian Ocean. Precipitation shows both continental and altitude effects, i.e. $\delta^2\text{H}$ and $\delta^{18}\text{O}$ are decreasing towards north with increasing distance from the Indian Ocean and increasing altitude from south to north, and values of $\delta^{18}\text{O}$ in geothermal waters also seem to be affected by a geothermal shift.

Results of reservoir temperature calculations based on the Na-Li geothermometer, (Fouillac and Michard, 1981), are shown in Table 5. At Rehoboth and Gross Barmen, calculated reservoir temperatures are the same as discharge temperatures, thus indicating a fast ascent of water. In contrast, the calculated temperature of 126 °C at Ganigobes differs significantly from other reservoir temperatures and the lower observed outflow temperature of 43.7 °C suggests a slow ascent towards discharge points with a gradual cooling of discharged water. This is also consistent with increased nitrate concentration at this site, suggesting mixing with shallow groundwater with resulting cooling of geothermal water. Estimated depths of circulation vary from 1210 m at Rehoboth to 3210 m at Ganigobis.

Concentrations of fluoride are high, with a maximum of 18.9 mg/l at Omapiyu and a minimum value of 2.13 mg/l at Ganigobes. Even the value at Ganigobes is higher than the WHO limit of 1.5 mg/l and Namibia's guideline value of 2 mg/l for water of good quality (NamWater, 2011). In all springs, except Ganigobes, water is supersaturated or close to saturation with the mineral fluorite. Concentrations of fluoride are similar to those at the Rift in Ethiopia, where 41.2% of samples show higher concentrations than the WHO limit (Rango et al., 2012; Tekle-Haimanot et al., 2006). In Ethiopia high fluoride levels are linked almost exclusively to the Na-HCO₃ type of water (Bretzler et al., 2011), i.e., water with low Ca concentrations, where equilibrium with respect to the mineral fluorite is not often reached. Also in the springs in Namibia, Na⁺ is the dominant cation, but waters south of Windhoek are rather of Na-HCO₃-SO₄ or Na-SO₄-HCO₃ type. A link between high fluoride and Na-HCO₃ type of water has been observed elsewhere in the world (Bhattacharya et al., 2006; Brunt et al., 2004). The input of

endogenous CO₂ is stipulated as a source of inorganic C in both Ethiopia and Namibia.

Primary source of fluoride cannot be determined with certainty, but it seems to be in magmatic rocks of the bedrock complex. For example, the Erongo granites developed at the Erongo complex in NW Namibia contain fluorite and beryl and the Damaran granite north of Okahandja also comprises abundant fluorite (Schneider, 2008). Fluoride minerals such as apatite were also found in deltaic sediments of the Cuvelai-Etoshia Basin in the north of Namibia (Dill et al., 2013). Micaceous can also be a source of fluoride because F[−] substitutes for OH[−] (Tischendorf et al., 2001).

Considering the high detected fluoride levels, some treatment method, e.g. bone char, contact precipitation, the Nalgonda method or Activated Alumina (e.g. Alarcón-Herrera et al., 2013), is necessary to decrease the dissolved fluorine to acceptable levels for drinking water purposes.

6. Conclusions

Investigation of geothermal springs in Namibia revealed high concentrations of dissolved fluorine, with values up to 18.9 mg/l. All values are higher than the WHO limit and the Namibian guideline. High concentrations of fluoride are linked to Na-HCO₃ or Na-HCO₃-SO₄ groundwater types, with increasing sulfate component towards the south. This is different from the Ethiopian Rift waters, where fluoride is linked to Na-HCO₃ waters. Concentrations of fluoride seem to be controlled by the precipitation of fluorite except for the Ganigobes sample.

Values of $\delta^2\text{H}$ and $\delta^{18}\text{O}$ become more negative towards the north with increasing altitude of the springs. This is a consequence of both a continental and altitude effect because air masses in Namibia originate in the southeast from the Indian Ocean area. There is a shift about 1‰ observed for $\delta^{18}\text{O}$ samples which may be caused by geothermal exchange with reservoir rocks. Values of $\delta^{34}\text{S}(\text{SO}_4)$ reflect mixing of two principal sulfate sources, i.e. dissolution of gypsum in playas and additional dissolution of sulfidic mineralization in tectonic bedrock zones. Values of $\delta^{13}\text{C}(\text{DIC})$ seem to be affected by a variable vegetation cover, and especially by the input of endogenous CO₂.

Estimated reservoir temperatures are from 60 °C to 126 °C, with a maximum at the Ganigobes site, where the ascent of water is probably slow and cooling takes place. Slight discrepancies (higher discharge compared to reservoir temperatures) at Rehoboth and especially at Ai-Ais are probably caused by a different geothermal gradient than that used for the calculations.

In summary, none of the studied geothermal springs of Namibia meets the drinking water standard and they can only be used for purposes such as in spas or heating.

Acknowledgements

The funding for this study was provided by the Czech Science Foundation (GACR P210/12/1413). Laboratory assistance by the following colleagues is gratefully acknowledged: L. Jílková (HPLC), V. Vonásková and M. Fayadová (major ions determination). We thank Kazimierz Rozanski from AGH Krakow for discussion about isotopes and Jiri

Table 5
Reservoir temperatures based on Na-Li geothermometer (Fouillac and Michard, 1981), depth calculated using geothermal gradient of 33 °C/km and average year temperature of 19.5 °C.

Spring	Rehoboth	Gross Barmen	Ganigobes	Omapiyu	Ai-Ais
Estimated temperature [°C]	60	70	126	85	67
Estimated depth of circulation [m]	1210	1510	3210	1965	1425
Observed outflow temp [°C]	60	48	43.7	47.4	60
Comment	Possibly higher geothermal gradient	Depth fits very well	Possibly uprising slowly and cooling	Possibly uprising slowly and cooling	Possibly higher geothermal gradient

Konopasek from University of Bergen for discussion about the origin of fluorine. We also thank two reviewers and associate editor for comments which helped to improve the manuscript.

References

- Alarcón-Herrera, M.T., Bundschuh, J., Nath, B., Nicolli, H.B., Gutierrez, M., Martín-Domínguez, I.R., Reyes-Gomez, V.M., Nuñez, D., Martín-Domínguez, A., Sracek, O., 2013. Co-occurrence of arsenic and fluoride in groundwater of semi-arid regions in Latin America: Genesis, mobility and remediation. *J. Hazard. Mater.* 262, 960–969.
- Armienta, M.A., Segovia, N., 2008. Arsenic and fluoride in the groundwater of Mexico. *Environ. Geochem. Health* 30, 345–353.
- Banks, D., Reimann, C., Røyset, O., Skarphagen, H., Sæther, O.M., 1995. Natural concentrations of major and trace elements in some Norwegian bedrock groundwaters. *Appl. Geochem.* 10, 1–16.
- Barsden, A., Bgorraton, K., Selving, K.A., 1996. Variability in fluoride content of sub-surface water reservoir. *Acta Odontol. Scand.* 54, 343–347.
- Bhattacharya, P., Claesson, M., Bundschuh, J., Sracek, O., Fagerberg, J., Jacks, G., Martin, R.A., del Stormiolo, A., Thir, J.M., 2006. Distribution and mobility of arsenic in the Río Dulce alluvial aquifers in Santiago del Estero Province, Argentina. *Sci. Total Environ.* 358, 97–120.
- Birkle, P., Bundschuh, J., Sracek, O., 2010. Mechanisms of arsenic enrichment in geothermal and petroleum reservoirs fluids in Mexico. *Water Res.* 44, 5605–5617.
- Bretzler, A., Osenbrück, K., Gloguen, R., Ruprecht, J.S., Kebede, S., Stadler, S., 2011. Groundwater origin and flow dynamics in active rift system – a multi-isotope approach in the Main Ethiopian Rift. *J. Hydrol.* 402, 274–289.
- Brunt, R., Vlasak, L., Griffioen, J., 2004. Fluoride in Groundwater: Probability of Occurrence of Excessive Concentration on Global Scale. IGRAC report, Utrecht. (12 pp.).
- Carillo-Rivera, J.J., Cardona, A., Edmunds, W.M., 2002. Use of abstraction regime and knowledge of hydrogeological conditions to control high-fluoride concentration in abstracted groundwater: San Luis Potosí basin, Mexico. *J. Hydrol.* 261 (1–4), 24–47.
- Chae, G.T., Yun, S.T., Kwon, M.J., Kim, S.Y., Mayer, B., 2006. Batch dissolution of granite and biotite in water: implication for fluorine geochemistry in groundwater. *Geochemistry* 40, 95–102.
- Clark, I., Fritz, P., 1997. *Environmental Isotopes in Hydrogeology*. Lewis Publishers, (328 pp.).
- Dill, H.G., Kaufhold, S., Lindenmaier, F., Dohrmann, R., Ludwig, R., Botz, R., 2013. Joint clay-heavy mineral analysis: a tool to investigate the hydraulic-hydrographic regime of Late Cenozoic Deltaic inland fans under changing climatic conditions (Cuvellai-Etosha Basin, Namibia). *Int. J. Earth Sci.* 102, 265–304.
- Dissanayake, C.B., Chandrajith, R., 2007. Medical geology in tropical countries with a special reference to Sri Lanka. *Environ. Geochem. Health* 29, 155–162.
- Dupalová, T., Sracek, O., Vencelides, Z., Žák, K., 2012. The origin of thermal waters in the northeastern part of the Eger Rift, Czech Republic. *Appl. Geochem.* 27 (3), 689–702.
- Eckhardt, F.D., Spiro, B., 1999. The origin of sulphur in gypsum and dissolved sulphate in the Central Namib Desert, Namibia. *Sediment. Geol.* 123 (3), 255–273.
- Fouillac, R., Michard, S., 1981. Sodium/Lithium ratio in water applied to geothermometry of geothermal reservoirs. *Geothermics* 10, 55–70.
- Gaciri, S.J., Davies, T.C., 1993. The occurrence and geochemistry of fluoride in some natural waters of Kenya. *J. Hydrol.* 143, 395–412.
- Gasse, F., 2000. Hydrological changes in the African tropics since the Last Glacial Maximum. *Quat. Sci. Rev.* 19, 189–211.
- Gizaw, B., 1996. The origin of high bicarbonate and fluoride concentration in Waters of the Main Ethiopian Rift Valley, East African Rift system. *J. Afr. Earth Sci.* 22, 391–402.
- Handa, B.K., 1975. Geochemistry and genesis of fluoride-containing groundwaters in India. *Groundwater* 13 (3), 275–281.
- Hem, J.D., 1992. Study and Interpretation of the Chemical Characteristics of Natural Water U.S. Geological Survey. Water Supply Paper 2254.
- Jacks, G., Bhattacharya, P., Chaudhary, V., Singh, K.P., 2005. Controls on the genesis of some high-fluoride groundwaters in India. *Appl. Geochem.* 20, 221–228.
- Johnson, R.B., Berg, M., Johnson, C.A., Tilley, E., Hering, J.G., 2011. Water and sanitation in developing countries: geochemical aspects of quality and treatment. *Elements* 7, 163–168.
- Kent, L.E., 1949. The Thermal Waters of the Union of South Africa and South West Africa. Transactions and proceedings of the Geological Society of South Africa vol. LII, pp. 231–264.
- Koritni, S., 1992. *Handbook of Geochemistry II/1*. Springer-Verlag, Berlin.
- Kundu, N., Panigrahi, M.K., Tripathy, S., Munshi, S., Powell, M.A., Hart, B.R., 2001. Geochemical appraisal of fluoride contamination of groundwater in the Nayagarh District of Orissa. *Indian Environ. Geol.* 41, 451–460.
- Lancaster, I.N., 1988. Development of linear dunes in the south-western Kalahari, southern Africa. *J. Arid Environ.* 14, 233–344.
- López, D.L., Bundschuh, J., Birkle, P., Armienta, M.A., Cumbal, L., Sracek, O., Cornejo, L., Ormachea, M., 2012. Arsenic in volcanic geothermal fluids of Latin America. *Sci. Total Environ.* 429, 57–75.
- McCrea, J.M., 1950. On the isotopic chemistry of carbonates and a paleotemperature scale. *J. Chem. Phys.* 18, 849–857.
- Miller, R.M., 2008. The Geology of Namibia vols. 1&2.
- Miller, R.M., 1983. The Pan-African orogen in South West Africa/Namibia. In: Miller, R.M. (Ed.), Evolution of the Damara Orogen of South West Africa/Namibia. Special Publ. Geol. Soc. S. Africa 11, pp. 431–512.
- Miller, R.M., 2008. The Geology of Namibia. Ministry of Mines and Energy, Geological Survey of Namibia.
- NamWater, 2011. Namibian water guideline: guideline for the evaluation drinking-water for human consumption with regard to chemical, physical and bacteriological quality.
- NEERI (National Environmental Engineering Research Institute, India), 1985. Fluoride, its incidence in natural water and de-fluoridation method.
- Noseck, U., Rozanski, K., Dulinski, M., Havlová, V., Sracek, O., Brassler, T., Hercik, M., Buckau, G., 2009. Carbon chemistry and groundwater dynamics at natural analogue site Ruprechtov, Czech Republic: insights from environmental isotopes. *Appl. Geochem.* 24, 1765–1776.
- Parkhurst, D.L., Appelo, C.A.J., 1999. User's Guide to PHREEQC; a Computer Program for Speciation, Reaction-path, 1-D Transport and Inverse Geochemical Calculations. U.S. Geological Survey Water Resources-Investigations Report 99–4259.
- Petzal, V.F.W., Schreiber, U.M., 1999. Simplified tectonostratigraphic map of Namibia. Geological Survey of Namibia.
- Pickering, W.F., 1985. The mobility of soluble fluoride in soils. *Environ. Pollut. B* 9, 281–308.
- Rango, T., Kravchenko, J., Atlaw, B., McCormick, P.G., Jeuland, M., Merola, B., Vengosh, A., 2012. Groundwater quality and its health impact: an assessment of dental fluorosis in rural inhabitants of the Main Ethiopian Rift. *Environ. Int.* 41, 37–47.
- Saxena, V.K., Ahme, S., 2001. Dissolution of fluoride in groundwater: a water-rock interaction study. *Environ. Geol.* 40, 1084–1087.
- Schneider, G., 2008. *The Roadside Geology of Namibia*, 2 Revised edition. (294 pp.).
- Shanyengana, E.S., Henschel, J.R., Seely, M.K., Sanderson, R.D., 2002. Exploring fog as a supplementary water source in Namibia. *Atmos. Res.* 64, 251–259.
- Sracek, O., Hirata, R., 2002. Geochemical and stable isotopic evolution of the Guarani Aquifer System in the state of São Paulo, Brazil. *Hydrogeol. J.* 10 (6), 643–655.
- Stute, M., Talma, A.S., 1998. Glacial temperatures and moisture transport regimes reconstructed from noble gases and $\delta^{18}\text{O}$. Stampriet Aquifer, Namibia. *Isotope Techniques in the Study of Environmental Change*. IAEA publications, pp. 307–318.
- Subba Rao, N., Devadas, D.J., 2003. Fluoride incidence in groundwater in an area of Peninsula India. *Environ. Geol.* 45, 243–251.
- Sudarshan, V., Rajeswara Reddy, B., 1991. Pollution of fluoride in ground water and its impact on environment and socio-economic status of the people – a case study in Sivannagudem area. *Indian J. Environ. Protect.* 11, 185–192.
- Talma, A.S., Vogel, J.C., 1983. O-18 variations of groundwater in southern Africa during the last 30,000 years. Abstracts of International Association of Meteorology and Atmospheric Physics (IAMAP), General Assembly, Hamburg 1983.
- Tekle-Haimanot, R., Melaku, Z., Kloos, H., Reiman, C., Fantaye, W., Zerihun, L., Bjortvan, K., 2006. The geographic distribution of fluoride in groundwater in Ethiopia with an emphasis on the Rift Valley. *Sci. Total Environ.* 367, 182–190.
- Tischendorf, G., Forster, H.-J., Gottesmann, B., 2001. Minor and trace element composition of trioctahedral micas: a review. *Mineral. Mag.* 65 (2), 249–276.
- Toran, L.E., Saunders, J.A., 1999. Modeling alternative paths of chemical evolution of NaHCO_3 -type groundwater near Oak Ridge, Tennessee, USA. *Hydrogeol. J.* 7 (1), 355–364.
- Webster, J.G., Nordstrom, D.K., 2003. Chapter 4. Geothermal arsenic. The source, transport and fate of arsenic in geothermal systems. In: Welch, A.H., Stollenwerk, K.G. (Eds.), *Arsenic in Groundwater: Geochemistry and Occurrence*. Kluwer.
- Wenzel, W.W., Blum, W.E.H., 1992. Fluoride speciation and mobility in fluoride contaminated soil and minerals. *Soil Sci.* 153, 357–364.
- WHO, 1998. Guidelines for drinking-water quality Appendix to 2nd ed. Health Criteria and Other Supporting Information vol. 2. World Health Organization, Geneva.
- Yanagisawa, F., Sakai, H., 1983. Thermal decomposition of barium sulphate for stable isotope analysis. *Anal. Chem.* 55, 985–987.